

CLAY MINERALS IN CAVES FROM NORTHWESTERN OLTEНИA

GHENCIU Monica

Abstract. X-ray diffraction data on 60 clay samples from the caves in the northwestern Oltenia, Cloșani, Ponoarele and Tismana areas, were analyzed using the X'Pert Quantify and X'Pert HighScore software. The following clay minerals were identified in the analyzed samples: illite, kaolinite, smectite, chlorite and vermiculite.

Keywords: clay minerals, caves, X-ray diffraction.

Rezumat. Mineralele argiloase în peșterile din nord-vestul Olteniei. Datele de difracție RX obținute pe 60 de probe de argilă prelevate din peșterile situate în nord-vestul Olteniei, zonele Cloșani, Ponoarele și Tismana, au fost analizate cu ajutorul programelor X'Pert Quantify și X'Pert HighScore. În probele analizate au fost identificate următoarele minerale argiloase: illit, caolinit, smectit, clorit și vermiculit.

Cuvinte cheie: minerale argiloase, peșteri, difracție RX.

INTRODUCTION

Most clays in the caves come from sediments and soils transported by the surface waters. Clays may appear as a subproduct of the limestones dissolution during the karstification process. The authigenic clay minerals formed under microclimatic conditions specific to the spelean environment, characterized by a constant temperature of 11-12 °C and a relative humidity of 100%, have been exhaustively described by HILL & FORTI (1997).

The region where the investigated caves are localized corresponds to the karst area in the northwestern Oltenia, representing the Mesozoic carbonate cover of the Danubian Realm. Most of the caves east of the Motru Valley are located in the limestone and dolomite massifs of Middle Jurassic-Neocomian age, predominantly consisting of micritic and pelmicritic carbonate rocks. West of the Motru Valley, most caves are located in massive organogenic limestone (Urgonian facies) of Barremian-Aptian age.

In the region to which we refer, DIACONU (1990) studied the clays from Cloșani Cave in which he identified kaolinite, illite and montmorillonite. For this paper, we collected 60 clay samples from 16 caves in the northeast Mehedinți Mountains (Cloșani area), the northeast Mehedinți Plateau (Ponoarele) and the southwest Vâlcan Mountains (Tismana area).

THE SAMPLING

The samples collected from the caves in the northwestern Oltenia are clays deposited on the cave floor, walls or fissures (45 samples), carbonate crusts inside the caves (10 samples) and soil from the immediate vicinity of the caves (5 samples). Their location and nature are presented below.

- Cloșani Cave (Mehedinți Mts.): 5 clay samples (CL_4, CL_7, CL_8, CL_10, CL_11) and 3 samples of carbonate crusts (CL_5, CL_6, CL_9).
- Cave No. 2 from Cloșani (Mehedinți Mts.): 4 clay samples (2CL_2, 2CL_4, 2CL_5, 2CL_6) and 2 samples of carbonate crusts (2CL_1, 2CL_3).
- Cave No. 5 from Coșani/Tunnel Cave (Mehedinți Mts.): 3 clay samples (TUN_1, TUN_2, TUN_3) and 1 sample of carbonate crust (TUN_4).
- Lazului Cave (Mehedinți Mts.): 3 clay samples (LAZ_6, LAZ_8, LAZ_9).
- Cave No. 9 on the Motru Sec Valley (Mehedinți Mts.): 2 clay samples (9MS_3, 9MS_4) and 2 soil samples (VMS_1, VMS_2).
- Cave No. 4 on the Lupșa Valley (Mehedinți Mts.): 2 clay samples (4VL_1, 4VL_2) and 1 soil sample (4VL_3).
- Cave No. 8 on the Lupșa Valley (Mehedinți Mts.): 3 clay samples (8VL_1, 8VL_2, 8VL_5) and 2 samples of carbonate crusts (8VL_3, 8VL_4).
- Cave No. 1 from Steiul Orzeștilor (Mehedinți Mts.): 1 clay sample (P1O_1) and 1 sample of carbonate crust (P2O_2).
- Cave No. 3 from Steiul Orzeștilor (Mehedinți Mts.): 1 clay sample (P1O_3).
- Cave from Ogașul Peșterii (Mehedinți Mts.): 4 clay samples (OP_1, OP_2, OP_3, OP_4).
- Cave from the Natural Bridge (Mehedinți Plateau): 3 clay samples (PN_1; PN_2, PN_6).
- Apa Moiștii Cave (Vâlcan Mts.): 2 clay samples (AM_1, AM_2).
- Fușteica Cave (Vâlcan Mts.): 6 clay samples (FUS_1, FUS_2, FUS_3, FUS_4, FUS_5, FUS_6).
- Red Cave from Piatra Pocruii (Vâlcan Mts.): 2 clay samples (PR_1, PR_2).
- Tihomir Cave (Vâlcan Mts.): 1 clay sample (TIH_2), 1 sample of carbonate crust (TIH_1) and 1 soil sample (TIH_3).
- Tismana Cave (Vâlcan Mts.): 3 clay samples (TM_1, TM_2, TM_3) and 1 soil sample (TM_4).

PRELIMINARY PHYSICO-CHEMICAL TREATMENTS

The determination of the mineralogical composition of the clay samples was done by X-ray diffraction on treated samples, under the following analytical conditions: Philips X'Pert diffractometer with CuK α radiation, step scanning 0.01, step time 1 s / step, scan interval 2 \div 40° 20.

It is generally believed that clay minerals are concentrated in the granulometric fraction <2 μ (e.g. MOORE & REYNOLDS, 1997), so that this mineralogical study refers exclusively to this fraction.

For an accurate determination of clay minerals by X-ray diffraction analysis, complex samples preparation is required in order to eliminate the impurities and increase the intensity of diffraction reflexes. Together with the clay minerals, non-clay minerals (quartz, feldspar, carbonates, Fe oxides) are commonly found in clays. Also, organic matter appears, which masks some 00l reflexes of the clay minerals. Most of these impurities were separated from the clay fraction by physico-chemical treatments.

The analyzed samples had a high content of organic matter and were treated with hydrogen peroxide 10% (KUNZE & DIXON, 1986) until its total removal. The carbonates were removed by treatment with 1M sodium acetate solution (RABENHORST & WILDING, 1984), followed by washing with distilled water to remove the calcium ions and possible water-soluble salts.

The separation of the clay fraction <2 μ was achieved by centrifugation of the slurry obtained after the removal of the organic matter and carbonates. To prevent the flocculation, Na pyrophosphate was added. To highlight the various clay minerals, we proceeded to the saturation of the samples in Mg²⁺ cations and ethylene glycol and to the heat treatment at 550° C (MOORE & REYNOLDS, 1997).

The obtained diffraction data was analyzed using the X'Pert Quantify and X'Pert HighScore softwares. The results were compared with data from the literature regarding the clay minerals identification (BISCAYE, 1964, BAILEY, 1980; MATEI, 1988; MOORE & REYNOLDS, 1997).

THE CLAY MINERALS IDENTIFICATION

Considering that highlighted clay phases may be members of solid solutions or mineral groups, we wanted to specify what each identified clay phase represents, as well as the characteristics obtained by X-ray diffraction. We used the term illite in the sense given by MOORE & REYNOLDS (1997) as the final member of a solid solution, due to the fact that the expandable interlayered structures present in proportions less than 5% in the solid solution cannot be highlighted by X-ray diffraction. The minor component is usually smectite or dioctahedral vermiculite.

Illite. It is the main mineral clay found in all samples based on the characteristic reflexes for the interplanar distances of 10.1 Å, 4.98-5.01 Å, 3.33 Å, and 2.89-2.92 Å. Illite shows a variation of the basal distance d(001) in the range of 9.88-10.12 Å. Treated with ethylene glycol, the illite does not expand. After heating at 550°C, the reflex (001) can slightly collapse (Fig 1). Values less than 10 Å can be attributed to the deficiency in K⁺ or to the substitution of Fe²⁺ and Mg²⁺ by [Al³⁺]_{IV} (GÜVEN et al., 1980). The illite polytypes could not be identified because of the presence of non-clay minerals that cause interferences of the diffraction reflexes. The illite diffraction data obtained on the analyzed samples, saturated in Mg²⁺ cations (Mg), saturated with ethylene glycol (EG) and heat treated at 550°C (T 550°C), are shown in Table 1.

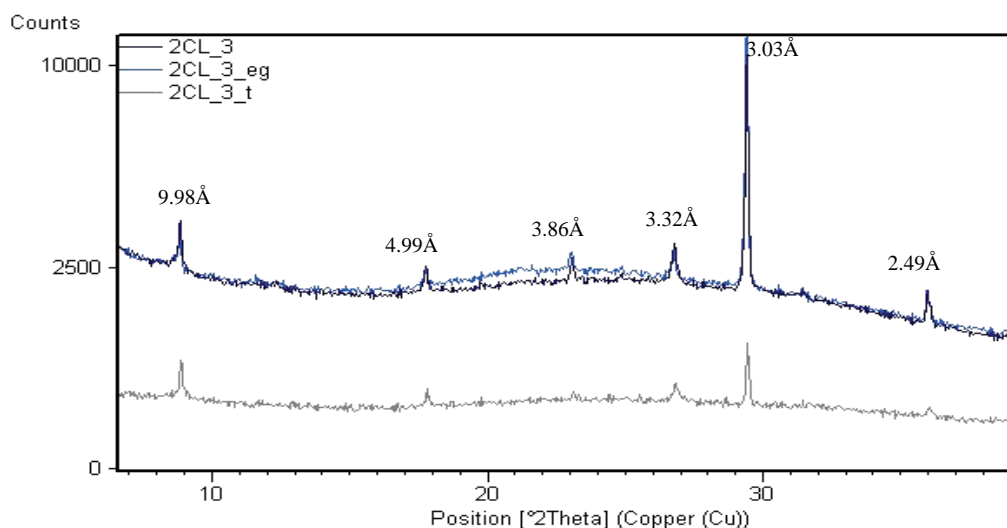


Figure 1. Diffractogram of 2CL_3 clay sample, in which the illite is present (without changes after ethylene glycol treatment and heat treatment).

Table 1. The illite X-ray diffraction data obtained on the analyzed samples.

No.	Sample	Mg			EG			T 550°C		
		d(001) Å	°2θ	Rel. Int (%)	d(001) Å	°2θ	Rel. Int (%)	d(001) Å	°2θ	Rel. Int (%)
1	CL_4	9.96	8.86	70.55	9.96	8.87	39.51	9.96	8.86	70.55
2	CL_5	10.06	8.78	20.13	10.05	8.79	31.53	9.93	8.89	13.16
3	CL_6	10.05	8.79	100.00	10.03	8.81	27.73	9.92	8.91	39.81
4	CL_7	10.11	8.74	49.46	10.05	8.79	59.30	9.87	8.95	80.35
5	CL_8	9.98	8.84	86.46	9.96	8.86	91.66	5.92	8.91	100
6	CL_9	10.08	8.76	71.41	10.07	8.77	57.64	9.97	8.86	28.95
7	CL_10	9.98	8.85	100.00	10.04	8.80	100.00	9.91	8.91	100
8	CL_11	10.01	8.83	48.57	9.99	8.84	38.78	9.93	8.90	83.59
9	2CL_1	10.02	8.82	96.42	10.00	8.83	100.00	9.95	8.88	100.00
10	2CL_2	9.93	8.90	100.00	9.97	8.86	84.65	9.98	8.85	95.56
11	2CL_3	9.98	8.85	12.76	10.00	8.83	9.84	9.95	8.88	59.19
12	2CL_4	10.07	8.78	45.82	10.04	8.80	97.59	9.97	8.86	51.01
13	2CL_5	9.98	8.85	100.00	9.97	8.86	52.53	9.96	8.87	100
14	2CL_6	10.12	8.73	100.00	10.09	8.75	100.00	9.98	8.86	79.99
15	TUN_1	9.99	8.84	100.00	10.04	8.80	100.00	9.97	8.86	100.00
16	TUN_2	10.01	8.83	98.08	9.99	8.85	55.03	9.98	8.85	100.00
17	TUN_3	10.06	8.78	42.43	10.09	8.76	79.07	9.95	8.88	100.00
18	TUN_4	9.98	8.85	35.47	9.98	8.85	21.56	10.03	8.81	87.64
19	LAZ_6	10.05	8.79	43.20	9.99	8.84	52.62	9.93	8.90	86.07
20	LAZ_8	10.00	8.84	96.34	10.01	8.82	40.48	9.92	8.90	85.55
21	LAZ_9	10.03	8.81	82.35	10.03	8.81	56.84	9.94	8.89	33.34
22	9MS_3	10.06	8.78	47.53	10.04	8.80	77.36	9.97	8.86	51.57
23	9MS_4	10.00	8.84	74.64	10.00	8.84	6.89	9.95	8.88	94.63
24	VMS_1	9.95	8.87	84.22	9.99	8.85	100.00	9.99	8.84	63.43
25	VMS_2	9.99	8.84	100.00	9.97	8.85	87.49	10.03	8.80	100.00
26	4VL_1	10.07	8.78	31.71	10.02	8.82	74.55	9.95	8.88	98.40
27	4VL_2	10.00	8.84	100.00	9.99	8.84	86.10	9.97	8.86	100.00
28	4VL_3	10.00	8.83	42.67	9.99	8.84	73.65	9.90	8.92	100.00
29	8VL_1	9.97	8.86	61.42	9.95	8.87	32.29	9.95	8.88	74.09
30	8VL_2	9.98	8.85	79.87	9.97	8.86	34.74	9.95	8.88	82.00
31	8VL_3	9.97	8.86	55.01	9.95	8.88	38.26	9.96	8.87	26.26
32	8VL_4	10.01	8.82	21.60	10.04	8.80	49.58	10.04	8.80	100.00
33	8VL_5	10.00	8.83	90.09	10.02	8.82	65.06	10.00	8.83	34.42
34	P1O_1	10.04	8.80	100.00	10.03	8.81	84.73	9.98	8.85	100.00
35	P2O_2	9.96	8.87	100.00	9.96	8.87	41.26	9.93	8.89	100.00
36	P2O_3	10.01	8.83	9.15	9.90	8.93	31.15	9.92	8.91	50.47
37	OP_1	10.04	8.79	100.00	9.97	8.85	77.47	9.96	8.87	53.69
38	OP_2	10.02	8.82	44.21	10.01	8.82	17.30	9.91	8.91	100.00
39	OP_3	10.04	8.80	31.57	10.04	8.74	33.32	10.03	8.81	71.65
40	OP_4	9.99	8.84	52.56	9.98	8.85	85.94			
41	PN_1	10.02	8.81	39.90	9.97	8.86	21.60	10.09	8.75	100.00
42	PN_3	9.99	8.84	31.86	9.98	8.86	22.41	10.02	8.82	100.00
43	PN_6	9.99	8.85	35.38	10.00	8.83	50.03	10.02	8.82	100.00
44	AM_1	9.97	8.86	33.72	10.00	8.84	48.34	9.97	8.86	100.00
45	AM_2	10.00	8.84	93.38	9.95	8.88	80.79	9.97	8.86	100.00
46	FUS_1	10.06	8.78	100.00	10.02	8.82	27.78	10.03	8.81	77.09
47	FUS_2	9.98	8.85	60.27	9.99	8.84	61.78	9.96	8.87	100.00
48	FUS_3	10.03	8.81	100.00	10.00	8.84	89.76	9.97	8.86	100.00
49	FUS_4	9.98	8.86	64.04	9.97	8.86	100.00	10.00	8.83	100.00
50	FUS_5	10.10	8.75	67.72	10.27	8.60	100.00	10.02	8.82	100.00
51	FUS_6	10.08	8.76	63.40	9.99	8.84	65.02	9.92	8.91	38.24
52	PR_1	9.88	8.94	37.44	9.86	8.96	17.79	9.97	8.86	48.43
53	PR_2	10.01	8.82	51.73	9.96	8.87	56.78	9.95	8.88	100.00
54	TIH_1	9.96	8.87	14.23	10.00	8.83	12.14	9.89	8.93	31.01
55	TIH_2	10.05	8.79	39.17	9.91	8.91	13.35	9.96	8.87	100.00
56	TIH_3	9.93	8.90	88.30	9.93	8.90	30.40	10.08	8.76	46.40
57	TM_1	9.94	8.89	53.49	9.97	8.86	50.80	10.01	8.82	100.00
58	TM_2	10.01	8.83	65.39	9.96	8.87	48.91	9.95	8.88	100.00
59	TM_3	9.97	8.86	38.42	10.00	8.84	40.19	9.97	8.86	100.00
60	TM_4	10.01	8.82	100.00	10.01	8.82	100.00	9.98	8.85	100.00

Kaolinite. This mineral is part of the same group as dickite, nacrite, halloysite 7 Å, and Halloysite 10 Å. Minerals certainly identified as kaolinite usually present varying degrees of disorder and it is considered that even halloysite is actually a kaolinite with a high degree of structural disorder (BRINDLEY, 1980).

Kaolinite is present in 59 of the analyzed samples. It was described on the basis of its basal reflex (001) at 7.06-7.14 Å and of (002) and (003) reflexes at 3.53 Å and 2.38 Å respectively, the latter making the difference between kaolinite and chlorite (BISCAYE, 1964).

The kaolinite in the analyzed samples has a basal distance $d(001)$ ranging between 7.08 and 7.23 Å (Mg-saturated samples) and does not swell by treatment with ethylene glycol. Due to the presence of vermiculite and chlorite, we paid attention to the reflex (003) at 2.38 Å. There are samples in which the reflex at 2.38 Å does not occur, although kaolinite is present and chlorite and vermiculite miss (e.g. the sample CL_10, Fig. 2). By heating at 550°C, the kaolinite becomes amorphous. The kaolinite diffraction data are shown in Table 2.

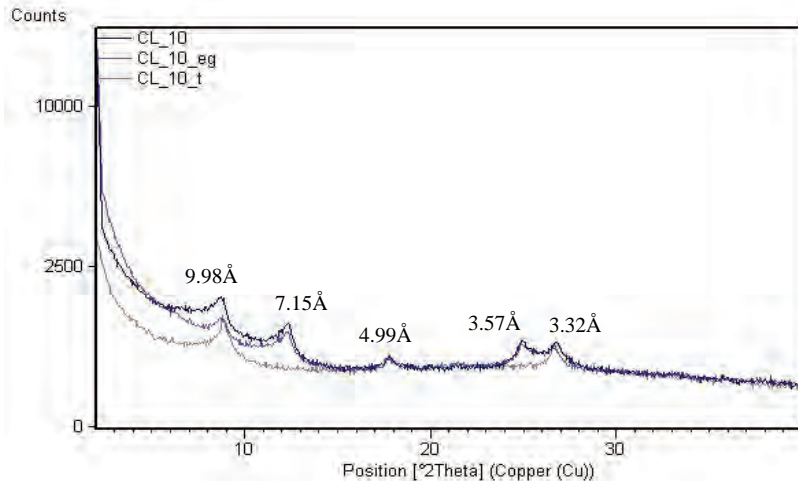


Figure 2. Diffractogram of CL_10 clay sample, in which the kaolinite is present (without changes after ethylene glycol treatment, with changes after heat treatment).

Table 2. The kaolinite X-ray diffraction data: $d(001)$ and $d(003)$ for samples treated with magnesium.

No.	Sample	Mg				
		$d(001)$ Å	$^{\circ}2\theta$	Rel. Int (%)	$d(003)$ Å	$^{\circ}2\theta$
1	CL_4	7.16	12.35	36.43	2.38	37.73
2	CL_5	7.21	12.26	14.07		
3	CL_6	7.19	12.30	68.21	2.38	37.69
4	CL_7	7.19	12.30	34.03	2.38	37.72
5	CL_8	7.14	12.38	55.79	2.37	37.78
6	CL_9	7.19	12.30	48.32	2.38	37.69
7	CL_10	7.15	12.37	64.44		
8	CL_11	7.15	12.37	100.00	2.38	37.76
9	2CL_1	7.17	12.33	100.00		
10	2CL_2	7.14	12.38	55.38	2.38	37.77
11	2CL_4	7.21	12.26	38.33	2.38	37.66
12	2CL_5	7.15	12.36		2.38	37.73
13	2CL_6	7.23	12.22	40.68		
14	TUN_1	7.16	12.36	76.22	2.38	37.78
15	TUN_2	7.16	12.53	68.19	2.38	37.66
16	TUN_3	7.21	12.26	25.10		
17	TUN_4	7.16	12.35	8.11		
18	LAZ_6	7.16	12.34	77.98	2.38	37.76
19	LAZ_8	7.18	12.32	61.52	2.38	37.69
20	LAZ_9	7.20	12.29	100.00	2.38	37.71
21	9MS_3	7.16	12.34	41.52	2.38	37.74
22	9MS_4	7.16	12.35	51.13	2.38	37.70
23	VMS_1	7.16	12.36	58.42		
24	VMS_2	7.14	12.38	42.91	2.38	37.75
25	4VL_1	7.14	12.38	21.93		
26	4VL_2	7.19	12.30	30.88	2.38	37.78
27	4VL_3	7.16	12.35	22.90	2.38	37.75
28	8VL_1	7.17	12.33	35.43	2.38	37.73
29	8VL_2	7.18	12.31	53.43	2.38	37.72
30	8VL_3	7.16	12.35	35.78	2.38	37.73
31	8VL_4	7.16	12.36	51.57	2.38	37.74
32	8VL_5	7.16	12.34	44.05	2.38	37.70
33	P1O_1	7.16	12.35	76.43		
34	P2O_2	7.15	12.37	88.13	2.38	37.77
35	P2O_3	7.18	12.32	24.54	2.38	37.74
36	OP_1	7.16	12.34	45.98	2.38	37.69
37	OP_2	7.20	12.28	100.00	2.38	37.71
38	OP_3	7.17	12.34	100.00	2.38	37.78

Table 2 (continued)

No.	Sample	Mg				
		d(001) Å	°2θ	Rel. Int (%)	d(003) Å	°2θ
39	OP_4	7.16	12.35	100.00	2.38	37.70
40	PN_1	7.17	12.33	100.00	2.38	37.72
41	PN_3	7.17	12.33	51.42		
42	PN_6	7.14	12.38	41.04	2.38	37.70
43	AM_1	7.15	12.37	67.55	2.38	37.76
44	AM_2	7.16	12.35	71.28	2.38	37.77
45	FUS_1	7.13	12.41	90.58		
46	FUS_2	7.16	12.35	55.12	2.38	37.73
47	FUS_3	7.16	12.35	50.21	2.38	37.76
48	FUS_4	7.17	12.34	100.00	2.38	37.75
49	FUS_5	7.20	12.27	100.00	2.38	37.67
50	FUS_6	7.15	12.37	100.00	2.38	37.68
51	PR_1	7.11	12.44	76.12	2.38	37.75
52	PR_2	7.16	12.35	53.35		
53	TIH_1	7.12	12.42	2.57		
54	TIH_2	7.20	12.28	26.85	2.38	37.73
55	TIH_3	7.13	12.39	67.23	2.38	37.76
56	TM_1	7.14	12.39	97.33	2.38	37.77
57	TM_2	7.08	12.50	48.77	2.37	37.84
58	TM_3	7.15	12.37	100.00	2.38	37.72
59	TM_4	7.15	12.36	41.88		

Smectite. Smectites are a group of minerals with both dioctahedral (e.g., montmorillonite) and trioctahedral (e.g. hectorite) structure. The main feature of their structure is the ability to expand or to contract without losing the crystallographic integrity. In order to highlight the smectitic species, detailed analyses are needed. In the absence of high resolution instrumental methods, the term smectite used in this work defines a clay phase with 2:1 type structure, dioctahedral and expandable.

The smectite was identified in 52 samples by comparing the reflex d(001) position in the clay samples treated with ethylene glycol with the reflex position in the clay samples saturated in Mg²⁺. Diagnostic reflexes of the smectite are at ~ 6° 2θ (14 Å) in the clays saturated with divalent ions (Mg²⁺) and at 5.2° 2θ (16.9 Å) in the clays saturated with ethylene glycol, as it can be seen in figure 3.

The smectite of the analyzed samples has a basal distance d(001) that varies between 13.97 Å and 14.95 Å (Mg-saturated samples) and swell by treating with ethylene glycol to form packages of thickness varying in the range 15.70-17.89 Å. By heat treatment at 550°C, the reflex (001) of smectite collapses at values of ~ 10 Å due to the complete release of the interlamellar water. The smectite diffraction data are shown in Table 3.

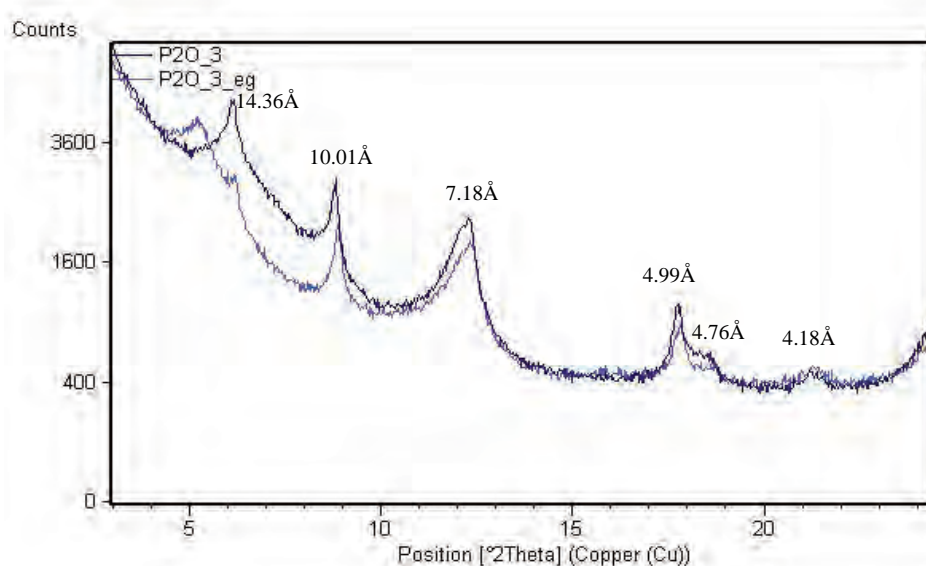


Figure 3. Diffractogram of P2O₃ clay sample, in which the smectite is present (with changes after ethylene glycol treatment).

Table 3. The smectite X-ray diffraction data obtained on the analyzed samples.

No.	Sample	Mg			EG		
		d(001) Å	°2θ	Rel. Int (%)	d(001) Å	°2θ	Rel. Int (%)
1	CL_4	14.46	6.11	80.57	16.49	5.35	31.99
2	CL_5	14.42	6.13	84.79	17.10	5.16	53.75
3	CL_6	14.45	6.11	42.02	17.06	6.14	11.00
4	CL_8	14.28	6.18	34.30		diffuse	
5	CL_9	14.05	6.28	100.00		diffuse	
6	CL_11	14.54	6.07	53.33	16.33	5.40	38.78
7	2CL_1	14.39	6.14	44.53		diffuse	
8	2CL_2	14.64	6.03	34.59		diffuse	
9	2CL_5	14.17	6.23	47.77	16.78	5.26	20.49
10	TUN_1	14.82	5.96	73.80		diffuse	
11	TUN_2	14.67	6.02	100.00	16.57	5.33	24.98
12	TUN_3	14.95	5.90	100.00	16.86	5.23	54.18
13	LAZ_6	14.40	6.13	100.00	16.80	5.25	46.83
14	LAZ_8	14.23	6.20	94.64	15.70	5.62	26.49
15	LAZ_9	14.05	6.28	81.32		diffuse	
16	9MS_3	14.30	6.17	49.31		diffuse	
17	9MS_4	14.42	6.12	84.06		diffuse	
18	VMS_1	14.03	6.29	28.21		diffuse	
19	VMS_2	14.17	6.23	47.14	16.86	5.30	64.12
20	4VL_1	14.31	6.17	100.00		diffuse	
21	4VL_2	14.23	6.20	39.87		diffuse	
22	4VL_3	14.46	6.11	100.00		diffuse	
23	8VL_1	14.20	6.22	100.00		diffuse	
24	8VL_2	14.24	6.20	100.00	16.76	5.27	44.71
25	8VL_3	14.17	6.23	37.20		diffuse	
26	8VL_4	14.19	6.22	100.00		diffuse	
27	8VL_5	14.41	6.13	100.00		diffuse	
28	P1O_1	14.45	6.11	14.65		diffuse	
29	P2O_2	14.19	6.22	42.71	16.92	5.22	21.71
30	P2O_3	14.36	6.15	100.00	16.74	5.27	100.00
31	OP_1	14.10	6.26	30.71		diffuse	
32	OP_2	14.22	6.21	23.26		diffuse	
33	OP_3	14.16	6.23	67.35		diffuse	
34	OP_4	14.16	6.24	50.19		diffuse	
35	PN_1	14.12	6.25	70.16	16.93	5.21	22.36
36	PN_3	14.31	6.17	100.00	17.00	5.19	100.00
37	PN_6	14.33	6.16	100.00	16.94	5.21	99.85
38	AM_1	14.26	6.19	100.00		diffuse	
39	AM_2	14.23	6.21	89.97		diffuse	
40	FUS_2	14.36	6.15	100.00		diffuse	
41	FUS_3	14.08	6.27	42.44		diffuse	
42	FUS_4	14.25	6.19	57.84		diffuse	
43	FUS_5	14.37	6.14	95.31		diffuse	
44	FUS_6	14.32	6.16	38.82	16.58	5.32	11.32
45	PR_1	14.16	6.23	100.00	15.99	5.52	32.17
46	PR_2	13.97	6.32	66.29		diffuse	
47	TIH_2	14.49	6.09	100.00	17.15	5.15	93.83
48	TIH_3	14.11	6.26	100.00		diffuse	
49	TM_1	14.16	6.23	58.29		diffuse	
50	TM_2	14.17	6.23	15.30	16.81	5.25	9.78
51	TM_3	14.11	6.26	57.74		diffuse	
52	TM_4	14.16	6.23	18.68		diffuse	

Chlorite. Most of the chloritic species have trioctahedral structures, i.e. both the octahedral layers are of trioctahedral type, but there may also be di-trioctahedral chlorites (e.g. sudoite). There is only one case of chlorite with two dioctahedral layers, the mineral being called dioctahedral chlorite. The chlorites exhibit wide compositional variations, the most common octahedral cations being Mg^{2+} , Fe^{2+} , Al^{3+} and Fe^{3+} .

The chlorite in the analyzed samples has a basal distance d(001) that varies between 14.03 Å and 14.49 Å (Mg-saturated samples) and does not swell by treating with ethylene glycol (Fig. 4). Heating for one hour at 550°C produces the dehydroxylation of the hydroxyl packages in the structure, which can be seen on diffractograms. The reflex (001) varies in the range 13.11-14.18 Å (6.13-6.73° 2θ); the other reflexes are weaker, but they do not disappear. Based on the thermal treatment, chlorite was identified in 14 samples. The chlorite diffraction data are shown in Table 4.

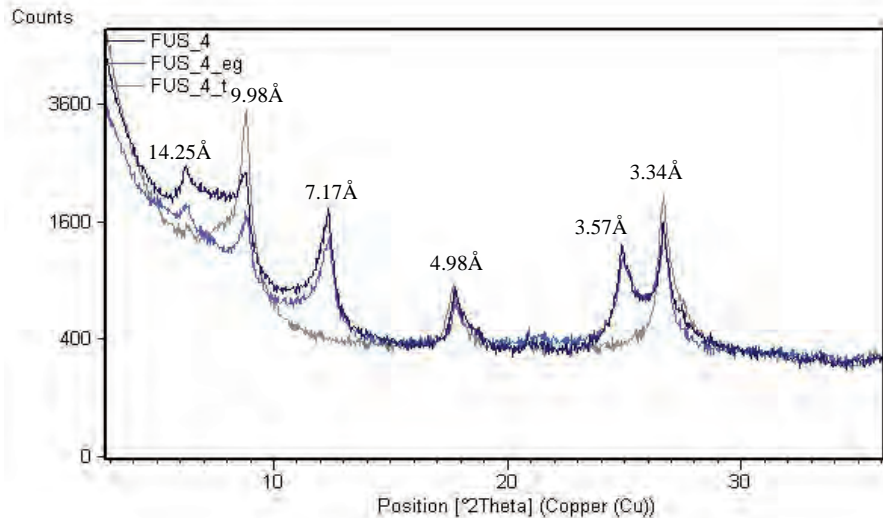


Figure 4. Diffractogram of FUS_4 clay sample, in which the chlorite is present (without changes after ethylene glycol treatment and heat treatment).

Table 4. The chlorite X-ray diffraction data obtained on the analyzed samples.

No.	Sample	Mg			EG			T 550°C		
		d(001) Å	°2θ	Rel. Int (%)	d(001) Å	°2θ	Rel. Int (%)	d(001) Å	°2θ	Rel. Int (%)
1	2CL_5	14.17	6.23	47.77	14.18	6.23	14.21	13.93	6.34	29.81
2	LAZ_6	14.40	6.13	100.00	14.10	6.26	62.48	13.86	6.37	9.48
3	VMS_1	14.03	6.29	28.21	14.09	6.26	14.29	13.96	6.32	8.89
4	VMS_2	14.17	6.23	47.14	14.27	6.18	43.70	14.18	6.23	64.63
5	4VL_2	14.23	6.20	39.87	14.27	6.19	15.23	13.98	6.13	15.56
6	8VL_3	14.17	6.23	37.20	14.02	6.30	29.97	13.76	6.42	14.46
7	8VL_5	14.41	6.13	100.00	14.22	6.21	26.12	13.79	6.40	36.32
8	P2O_2	14.19	6.22	42.71	14.15	6.24	7.49	13.11	6.73	34.25
9	P2O_3	14.36	6.15	100.00	14.31	6.17	61.97	13.59	6.50	24.90
10	AM_1	14.26	6.19	100.00	14.16	6.24	51.22	13.89	6.36	7.99
11	FUS_4	14.25	6.19	57.84	14.02	6.30	58.17	13.89	6.35	5.81
12	TIH_2	14.49	6.09	100.00	15.49	5.70	54.37	13.81	6.39	50.33
13	TIH_3	14.11	6.26	100.00	14.16	6.24	55.89	14.18	6.23	33.66
14	TM_2	14.17	6.23	15.30	14.13	6.25	10.03	14.07	6.28	14.62

Vermiculite. Among the clay minerals, vermiculite is the most difficult phase to identify because of its variable characteristics.

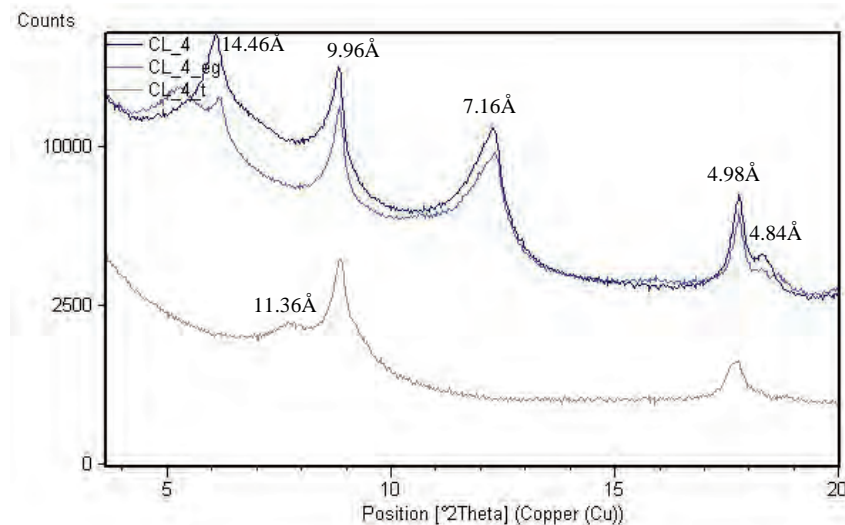


Figure 5. Diffractogram of CL_4 clay sample, in which the vermiculite is present (without changes after ethylene glycol treatment, with changes after heat treatment).

Vermiculite can be regarded as a member of different compositional series: biotite-trioctahedral vermiculite-trioctahedral smectite, muscovite-dioctahedral vermiculite-dioctahedral smectite, and chlorite-vermiculite (very likely both dioctahedral). Depending on its origin, vermiculite usually contains interlayers with phyllosilicate structures belonging to the

precursors, i.e. biotite/vermiculite, illite/vermiculite or smectite/vermiculite. The smectite/vermiculite interlayers are probably frequent, due to the structural similarities of the two minerals, but their nature is not yet well established.

Vermiculite recognition in the analyzed samples is difficult because of its coexistence with chlorite and kaolinite. The reflex (001) of vermiculite is found at $\sim 7^\circ 2\theta$ (14.4 \AA). It can be highlighted by treating the samples with ethylene glycol that makes the smectitic packages to expand at $\sim 17 \text{ \AA}$. After heating at 400°C and 550°C , the reflex (001) of the dioctaedic vermiculite collapses to nearly 12 \AA and 11 \AA , respectively. Vermiculite can also be differentiated based on the reflex (060) at 1.50 \AA (dioctahedral vermiculite) and at $1.52\text{-}1.54 \text{ \AA}$ (trioctahedral vermiculite) (DOUGLAS, 1989).

The vermiculite was identified in 46 samples, 18 of them containing dioctahedral vermiculite (Fig. 5). The vermiculite diffraction data are shown in Table 5.

Table 5. The vermiculite X-ray diffraction data obtained on the analyzed samples.

No.	Sample	Mg			EG			T 550°C		
		d(001) Å	$^{\circ}2\theta$	Rel. Int (%)	d(001) Å	$^{\circ}2\theta$	Rel. Int (%)	d(001) Å	$^{\circ}2\theta$	Rel. Int (%)
1	CL_4	14.46	6.11	80.57	14.26	6.19	20.77	11.36	7.77	46.69
2	CL_5	14.42	6.13	84.79	14.28	6.18	49.53			
3	CL_6	14.45	6.11	42.02	14.38	6.14	11.00			
4	CL_8	14.28	6.18	34.30	14.15	6.25	21.64			
5	CL_9	14.05	6.28	100.00	14.21	6.21	77.20			
6	2CL_2	14.64	6.03	34.59	14.40	6.13	19.72			
7	2CL_5	14.17	6.23	47.77	14.18	6.23	14.21			
8	TUN_2	14.67	6.02	100.00	14.35	6.15	27.94			
9	TUN_3	14.95	5.90	100.00	14.98	5.89	37.47			
10	LAZ_6	14.40	6.13	100.00	14.10	6.26	62.48	11.90	7.42	60.06
11	LAZ_9	14.05	6.28	81.32	14.13	6.25	71.37			
12	9MS_3	14.30	6.17	49.31	14.24	6.20	15.17			
13	9MS_4	14.42	6.12	84.06	14.13	6.25	34.61	11.86	7.45	100
14	VMS_1	14.03	6.29	28.21	14.09	6.26	14.29	11.87	7.44	29.26
15	VMS_2	14.17	6.23	47.14	14.27	6.18	43.70	12.01	7.35	83.72
16	4VL_2	14.23	6.20	39.87	14.27	6.19	15.23	12.04	7.34	62.49
17	4VL_3	14.46	6.11	100.00	14.18	6.23	73.26	11.50	7.68	75.34
18	8VL_1	14.20	6.22	100.00	14.02	6.30	39.05	11.75	7.52	100.00
19	8VL_2	14.24	6.20	100.00	14.15	6.24	60.48	11.55	7.65	100.00
20	8VL_3	14.17	6.23	37.20	14.02	6.30	29.97	11.83	7.47	69.31
21	8VL_4	14.19	6.22	100.00	14.37	6.15	98.58			
22	8VL_5	14.41	6.13	100.00	14.22	6.21	26.12	11.72	7.53	100.00
23	P2O_2	14.19	6.22	42.71	14.15	6.24	7.49			
24	P2O_3	14.36	6.15	100.00	14.31	6.17	61.97			
25	OP_1	14.10	6.26	30.71	14.19	6.23	14.08	11.61	7.61	34.12
26	OP_2	14.22	6.21	23.26	14.12	6.25	11.97	11.66	7.58	94.18
27	OP_3	14.16	6.23	67.35	14.11	6.26	29.76	11.62	7.6	43.55
28	OP_4	14.16	6.24	50.19	14.16	6.23	40.16			
29	PN_1	14.12	6.25	70.16	14.17	6.23	18.35	11.91	7.42	32.16
30	PN_3	14.31	6.17	100.00	14.19	6.22	44.98	11.98	7.37	42.29
31	PN_6	14.33	6.16	100.00	14.12	6.25	40.24	11.99	7.37	33.42
32	AM_1	14.26	6.19	100.00	14.16	6.24	51.22			
33	AM_2	14.23	6.21	89.97	14.27	6.19	87.67			
34	FUS_2	14.36	6.15	100.00	14.18	6.23	41.91			
35	FUS_3	14.08	6.27	42.44	14.18	6.22	40.24			
36	FUS_4	14.25	6.19	57.84	14.02	6.30	58.17			
37	FUS_5	14.37	6.14	95.31	14.66	6.02	49.63			
38	FUS_6	14.32	6.16	38.82	14.11	6.26	21.62			
39	PR_1	14.16	6.23	100.00	14.25	6.20	27.12			
40	PR_2	13.97	6.32	36.43	14.06	6.28	45.63			
41	TIH_2	14.49	6.09	100.00	15.49	5.70	54.37	11.98	7.37	93.58
42	TIH_3	14.11	6.26	100.00	14.16	6.24	55.89			
43	TM_1	14.16	6.23	58.29	14.35	6.15	36.78			
44	TM_2	14.17	6.23	15.30	14.13	6.25	10.03			
45	TM_3	14.11	6.26	57.74	14.30	6.17	18.45			
46	TM_4	14.16	6.23	18.68	14.29	6.18	13.26			

Non-clay minerals. In the analyzed samples, there are also non-clay minerals that could not be completely separated because of the small size of the crystals. The quartz was identified based on the reflexes at 4.25 and 3.34 \AA , and the potassium feldspar by the presence of the reflex at 3.24 \AA . In one sample, it was identified pyrophyllite, based on the reflex at 9.20 \AA ($8.84^\circ 2\theta$). Carbonates, incompletely dissolved by acetic acid treatment, were also identified based on the reflexes at 3.03 \AA (calcite) and 2.88 \AA (dolomite).

CONCLUSIONS

In this study, there were analyzed by X-ray diffraction the clay minerals from 60 samples collected from 16 different caves. The following minerals were identified in all samples: illite (60 samples), kaolinite (59 samples), smectite (52 samples), chlorite (14 samples) and vermiculite (46 samples, 18 of which dioctahedral vermiculite). These minerals occur in both the clay samples as well as the carbonate crusts and soil samples.

The clay minerals from the spelean environment can be relevant for identifying the sediments source area and for knowledge of the erosion processes and evolution of the caves in the region, as we will try to do in a future work.

REFERENCES

- BAILEY S. W. 1980. Summary and recommendations of AIPEA nomenclature committee. *Clays and Clay Minerals.* The Clay Minerals Society. **28:** 73-78.
- BISCAYE P. E. 1964. Distinction between kaolinite and chlorite in recent sediments by X-ray diffraction. *American Mineralogist.* Mineralogical Society of America. **49:**1282-1289.
- BRINDLEY G. W. 1980. Order-disorder in clay mineral structures. In Brindley G. W. & Brown G. (Eds.): *Crystal Structures of Clay Minerals and their X-ray Identification.* Mineralogical Society. London: 125-196.
- DIACONU G. 1990. Closani cave. Mineralogical and genetic study of carbonates and clays. *Miscellanea speologica romanica.* Institute of Speleology "Emil Racoviță". București. **2:** 3-194.
- DOUGLAS L. A. 1989. Vermiculites. In Dixon J. B. & Weed S. B. (Eds.): *Minerals in soil environments.* 2nd Edition. Soil Science Society of America Book Series. Madison: 625-674.
- GÜVEN N., HOWER W. F., DAVIES D. K. 1980. Nature of authigenic illites in sandstone reservoirs. *Journal of Sedimentary Petrology.* Society of Economic Paleontologists and Mineralogists. **50:** 761-766.
- HILL C. A. & FORTI P. 1997. *Cave Minerals of the World.* 2nd Edition. National Speleological Society. Huntsville. 463 pp.
- KUNZE G. W. & DIXON J. B. 1986. Pretreatment for mineralogical analysis. In A. Klute (Ed.): *Methods of soil analysis. Part 1: Physical and Mineralogical methods,* 2nd Edition. American Society of Agronomy/Soil Science Society of America. Madison: 91-100.
- MATEI L. 1988. *Determinator pentru metode fizice de analiză a mineralelor și rocilor.* University of Bucharest Printing House. 363 pp.
- MOORE D. & REYNOLDS R. C. 1997. *X-Ray Diffraction and the Identification and Analysis of Clay Minerals,* 2nd Edition. Oxford University Press. New York. 378 pp.
- RABENHORST M. C. & WILDING L. P. 1984. Rapid method to obtain carbonate-free residues from limestones and petrocalcic materials. *Soil Science Society of America journal.* Soil Science Society of America. **48:** 216-219.

Ghenciu Monica
Geological Institute of Romania,
1st Caransebeș Street, 012271 - Bucharest, Romania.
E-mail: monica_ghenciu@yahoo.com

Received : March 8, 2017
Accepted: August 6, 2017